

# Characterization of the Kinetic Phase Transition of Phospholipids Using Avrami and Tobin Models

CHEN, Lin<sup>a</sup> (陈琳)    YU, Zhi-Wu<sup>\*·a</sup> (尉志武)    XUE, Fang-Yu<sup>b</sup> (薛芳渝)  
HONG, Xiao-Yin<sup>b</sup> (洪啸吟)

<sup>a</sup> Bioorganic Phosphorous Chemistry Laboratory, Tsinghua University, Beijing 100084, China

<sup>b</sup> Department of Chemistry, Tsinghua University, Beijing 100084, China

Mechanism of the lamellar crystalline phase formation of distearoyl-phosphatidylethanolamine (DSPE) dispersed in excess glycerol has been examined by differential scanning calorimetry. It was found that transformation of liquid-crystal phase to a crystalline phase must be mediated by a lamellar-gel phase. Further examination of the kinetic phase behavior using Avrami and Tobin models suggested a single dimensional growing pattern and a three-step mechanism of the crystallization, consisting of nucleation, normal growth, and restricted growth.

**Keywords** DSPE, crystallization, Avrami equation, Tobin model, glycerol, DSC

## Introduction

Phase segregation in biomembranes is believed to be the first step of cryoinjury when living organisms are subjected to low temperatures.<sup>1</sup> On the other hand, domain formation in membrane lipid matrix has also been proved to play a crucial role in proper functioning of living cells.<sup>2</sup> Among many questions remaining in the area of lipid phase transitions, a hot topic has been the mechanism of the formation of crystalline phases within lipid dispersion.<sup>3-5</sup>

As a naturally occurring osmoticant in some species and a widely used cryoprotectant,<sup>6-7</sup> glycerol has been investigated in the context of its modulation effect on the phase behaviour of phospholipids.<sup>8-10</sup> Of the two main

categories of phospholipids, *i. e.* the bilayer-forming phosphatidylcholines and nonbilayer-forming phosphatidylethanolamines, it has been shown that glycerol can induce interdigitated phase in the former<sup>8</sup> and favors the formation of inverted hexagonal phase ( $H_{II}$ ) and crystalline phases of the latter.<sup>10</sup> As a representative of the latter, distearoylphosphatidylethanolamine (DSPE) shows two thermodynamically stable phases when dispersed in pure glycerol, *i. e.* the crystalline phase  $L_c$  at low temperatures and  $H_{II}$  at high temperatures. These two phases, together with a lamellar-gel phase ( $L_\beta$ ) and a less stable lamellar-crystalline phase ( $L_c$ ), have been characterized in our previous study using X-ray diffraction method.<sup>10</sup> Upon heating, a first-order phase transition from  $L_c$  to  $H_{II}$  can be demonstrated unambiguously. The reverse process, however, is still problematic. In this article, we will first clarify the conditions of the formation of crystalline phases, then make a comparison of Avrami and Tobin models in describing the kinetics of the transition.

## Experimental

Synthetic 1, 2-distearoyl-*sn*-phosphatidylethanolamine (DSPE), with a purity better than 99%, was purchased from Sigma Chemical Co. (St. Louis, MO). Glycerol was purchased from Beihua Fine Chemicals (Beijing, China) and was of AR grade. Samples were

\* E-mail: yuzhw@mail.tsinghua.edu.cn

Received December 18, 2000; revised March 29, 2001; accepted April 3, 2001.

Project supported by the National Natural Science Foundation of China (No. 29973019) and partially by a fund from the key-faculty supporting scheme of the Ministry of Education of China.

prepared by dispersing DSPE in glycerol with a mass ratio of 1:10 to 1:15 to guaranty an excess of solvent. In order to eliminate any effects of thermal history, dispersions were maintained at 100°C for 60 min, which is greater than the fluid phase formation temperature. A Mettler-Toledo DSC821e differential scanning calorimeter (DSC) was used to examine phase behavior of the lipid dispersions. The signal time constant is 3 seconds, resolution is better than 0.7  $\mu$ W, and noise (RMS) is less than 1  $\mu$ W.

A T-jump protocol was used to study the kinetics of crystalline phase formation at different incubation temperatures to minimize the growth of nuclei during heating from nucleation temperature to incubation temperature. After being treated at 100°C, lipid dispersions were first cooled to 65°C at a rate of 5°C/min to allow nucleation. Then the temperature of each sample pan was jumped to a higher temperature for the isothermal incubation measurement. The heating rate of this T-jump was greater than 100°C/min.

Avrami model<sup>11,12</sup> and Tobin model<sup>13-15</sup> were used in the present study to elucidate the kinetic mechanism of crystalline phase formation. By assuming that the evolution of the crystallinity is linearly proportional to the evolution of heat released during isothermal crystallization in the DSC pans, the relative transition fraction  $\theta(t)$  can thus be calculated by integration of the crystallization exothermic curves according to Eq. (1). The Avrami equation can be written as Eq. (2) or (3)

$$\theta = \int_0^t \frac{dH_t}{dt} dt / \int_0^{\infty} \frac{dH_t}{dt} dt \quad (1)$$

$$\theta = 1 - \exp[-(k_a t)^n] \quad (2)$$

$$\ln[-\ln(1 - \theta)] = n \ln k_a + n \ln t \quad (3)$$

where  $\theta$  denotes the transition fraction as a function of time,  $k_a$  is the Avrami crystallization rate constant,  $n$  is the Avrami exponent, a parameter related to the crystal growth morphology. According to the original assumption of the theory, the value of  $n$  should be an integer from 1 to 4.<sup>16</sup> It is worth noting that the Avrami equation is only applicable to the early stage of crystallization, but not to the late stage process because the Avrami model does not take account of the conflict of neighboring crystalline do-

main when the growing rate is significantly reduced. To solve the problem, Tobin proposed a different model as shown in Eq. (4) or (5).

$$\theta = (k_i t)^n / [1 + (k_i t)^n] \quad (4)$$

$$\ln \theta - \ln(1 - \theta) = n \ln t + n \ln k_i \quad (5)$$

The Tobin exponent  $n$  may not be integer.<sup>15</sup> Parameters of both models can be derived from the least-square linear regression according to Eq. (3) and (5), respectively.

## Results and discussion

### Mechanism of the formation of crystalline phases

Shown in Fig. 1 (curve a) is the phase transition of a DSPE dispersion, after long time storage under 4°C, from the most stable lamellar-crystalline phase ( $L_c$ ) to the inverted hexagonal phase ( $H_{II}$ ). The transition temperature and enthalpy is 88.4°C and 120 J/g, respectively. Upon cooling at a rate of 5°C/min, however,  $H_{II}$  transforms into another lamellar phase  $L_{\beta}$  (curve b) at 74.9°C. The hysteresis between the two transitions is more than 13 degrees.

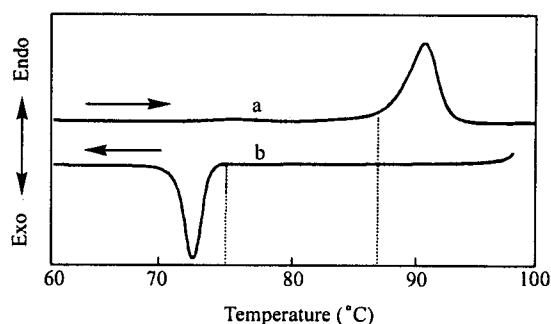


**Fig. 1** DSC curves of a DSPE dispersion in glycerol, showing transition from lamellar-crystalline  $L_c$  phase to inverted hexagonal phase ( $H_{II}$ ) upon heating (curve a) and transition from  $H_{II}$  to lamellar-gel phase upon cooling (curve b). The scanning rate was 5°C/min.

To elucidate the mechanism of the formation of  $L_c$  phase, thermal measurement at different heating/cooling rates and isothermal incubation at different temperatures below 88.4°C has been performed. Shown in Fig. 2A is

the DSC curve of an incubation measurement at 75.3°C after the sample was cooled from 100°C at a rate of 5°C/min. The overall enthalpy of the double peaks, 100 J/g, indicates that the final phase is not the most stable  $L_c$  phase. The sharp peak is assigned as the phase transition from  $H_{II}$  to  $L_\beta$ .<sup>10</sup> The other was explained as the transformation from  $L_\beta$  to the less stable crystalline phase  $L_c'$  because the subsequent heating, as shown in Fig.

2B, resulted in a typical endotherm-exotherm-endotherm transformation pattern.<sup>10</sup> Such pattern is the result of a partial endothermic transformation from  $L_c'$  to  $H_{II}$ , followed by an exothermic relaxation of  $L_c'$  to  $L_c$  and another endothermic transformation from  $L_c$  to  $H_{II}$ . Isothermal incubation at other temperatures ranging from 68.8 to 76.3°C showed similar phase transitions.

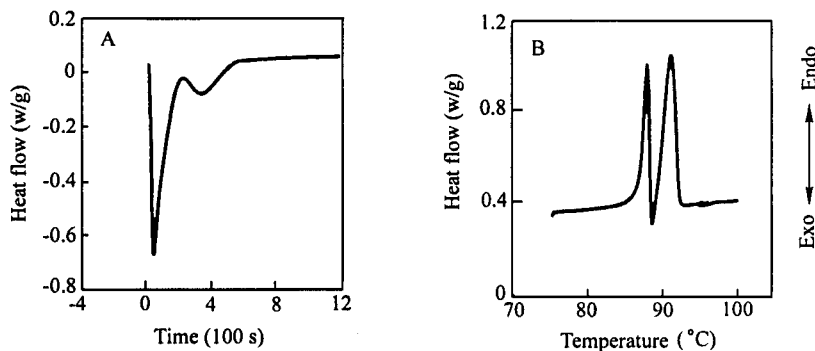


Fig. 2 DSC curves of a DSPE dispersion during isothermal incubation at 75.3°C (A) and the subsequent heating at a rate of 1°C/min (B).

A conclusion can be drawn from these results is that the  $L_c'$  can not form directly from the  $H_{II}$  phase. The latter must first transform into a metastable solid phase  $L_\beta$  before it can further relax to  $L_c'$ . This is understandable because lower temperature usually favors nucleation process,<sup>3</sup> while the possibility to form very ordered crystalline nuclei within the fluid  $H_{II}$  phase is very limited.

Incubation of  $L_\beta$  phase at temperatures lower than 68.8°C did not result in detectable  $L_c'$  phase with the calorimeter. This may be due to the slow growing rate of the nuclei at low temperatures. To rearrange molecules in a solid state requires energy, or activation energy.<sup>17</sup> This is actually the reason that only significant growing rate was observed at temperatures greater than 68.8°C using the DSC method. In addition, both cooling and heating with a rate less than 1°C/min at temperatures between 68 and 76°C can also cause measurable relaxation of  $L_\beta$  to  $L_c'$ .

To clarify the formation conditions of the  $L_c$  phase, samples have been heated to 100°C after different thermal treatment at temperatures lower than ca. 85°C. Similar DSC curves like that in Fig. 2B were obtained in each case with overall enthalpies of about 100 J/g. This indicates that the formation of  $L_c$  structures at low temperatures, if there is any, is insignificant. Only incuba-

tion of the DSPE dispersion at about 87°C can induce the formation of the most stable  $L_c$  phase.

#### Kinetics of the crystalline phase formation

Temperatures higher than 68.8°C can promote the growth of  $L_c'$  phase significantly. To collect the kinetic data of the growth of the  $L_c'$  nuclei, a DSPE dispersion was T-jumped to an incubation temperature between 72 and 76°C after the sample was cooled first to 65°C at a rate of 5°C/min. Shown in Fig. 3A is a representative DSC curve of the exotherm phase transition from  $L_\beta \rightarrow L_c'$  recorded at 72°C. The time sequence of the fractional transformation as calculated from Eq. (1) is depicted in Fig. 3B.

The Avrami plot of the data from Fig. 3B, in a form of  $\ln(-\ln(1-\theta))$  versus  $\ln t$ , is shown in Fig. 4. The deviation of the secondary stage (line b) from the primary stage linearity (line a) may arise from the intrinsic shortcoming of Avrami model, in which the impingement of nuclei is not considered at late stage of crystallization. Parameters of the exponent  $n$  and rate constant  $k_a$  at 72°C and other temperatures were thus calculated from the slope and intercept of least-square regression using the data at the primary stage of the

transformation only. Activation energy can thus be obtained from the relationship between  $\ln(k_a)$  and  $1/T$  using Arrhenius equation. These parameters and the fitting correlation coefficients are listed in Table 1. Activation energies obtained in this study are very close to the

energy of dipalmitoylphosphatidylcholine during the main phase transition from  $L_\beta$  to  $L_\alpha$ , which was found to be about 211 kJ/mol by the turbidity measurement.<sup>18</sup> Activation energy of the  $L_\beta$  to  $L_c$  phase transition can be interpreted as the energy of the nuclei formation.

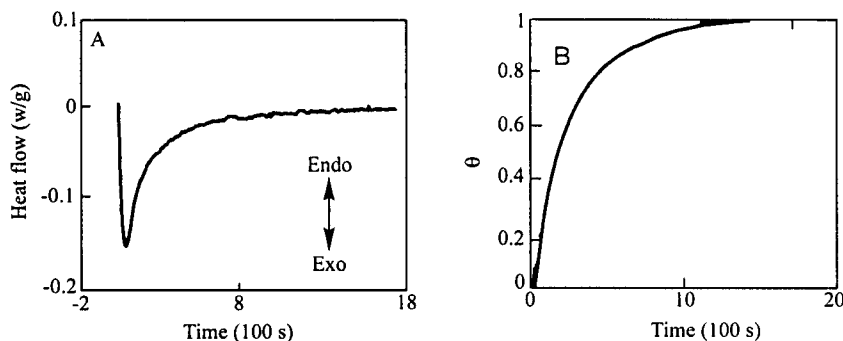


**Fig. 3** Isothermal transformation of lamellar-gel to lamellar-crystalline phase  $L_c$  (A) and the plot of phase transition fraction  $\theta$  versus time at  $72^\circ\text{C}$  (B). See text for details.

**Table 1** Exponents and rate constants of Avrami equation and Tobin equation for the isothermal phase transition of DSPE in excess glycerol at different temperatures

$T$ ( $^\circ\text{C}$ )	Avrami model				Tobin model			
	$n$	$\ln k_A$	$E_A$ (kJ/mol)	$r_A^a$	$n$	$\ln k_T$	$E_T$ (kJ/mol)	$r_T^a$
72	1.59	-4.89	205.9	0.9726	1.58	-5.06	179.9	0.9396
73	1.56	-4.74			1.60	-4.99		
74	1.55	-4.50			1.33	-4.82		
75	1.64	-4.22			1.44	-4.65		
76	1.71	-4.12			1.23	-4.33		
Average	$1.61 \pm 0.07$				$1.44 \pm 0.16$			

<sup>a</sup>  $r_A$  and  $r_T$ : linear correlation coefficients obtained by Avrami model and Tobin model, respectively;

$E_A$  and  $E_T$ : apparent activation energies obtained by Avrami model and Tobin model, respectively.

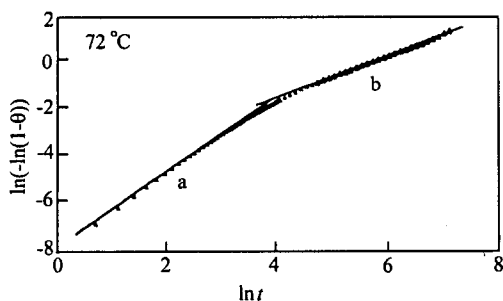


**Fig. 4** Avrami plots of data shown in Fig. 3B, showing the growing kinetics deviation of the secondary stage from the primary stage.

To further understand the growing mechanism of the crystalline phase, Tobin model has also been employed to describe the phase transition kinetics. This model is

different from the Avrami model in that it has taken account of the size impingement during the growing process of crystallization.<sup>16</sup> Illustrated in Fig. 5 is an example of the Tobin plot using data from Fig. 3B. The exponent  $n$  and the rate constant  $k_t$  derived from the linear least-square regression at different temperatures are listed also in Table 1. It is thus clear that Tobin model gives a much better description of the crystallization process of the lipid dispersion than Avrami model. This can further be seen from the predicted transition progress curves of both models as shown in Fig. 6. All these indicate that the crystallization process is in agreement with a three-step mechanism consisting of nucleation, normal growth, and restricted growth due to impingement.

The apparent exponents derived from both models

are about 1.61 and 1.44, respectively. Due to the fact that both nucleation and growth can happen at the measuring temperatures (see Fig. 2A, for example), the exponent value should be reduced by 1.<sup>4</sup> This gives an effective growth dimensionality of one, following the reasoning of Cheng and Caffrey, where the Avrami exponent was found to be between 0.7 and 0.9 for the order-to-disorder conformational transformation of monoelaidin dispersed in water.<sup>5</sup> The most likely attribution to this dimension is the direction perpendicular to the lamellar plane, because the growth of nuclei in the lamellar plane must be faster than that in the layer-by-layer direction.<sup>19</sup>

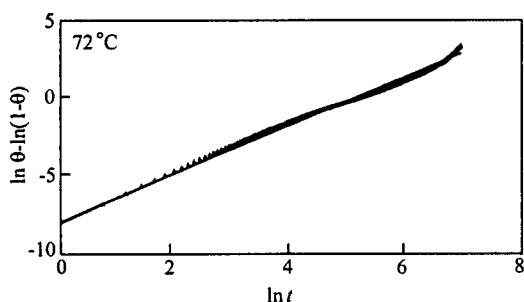


Fig. 5 Tobin plots of data shown in Fig. 3B calculated according to the Tobin relationship of the transformation.

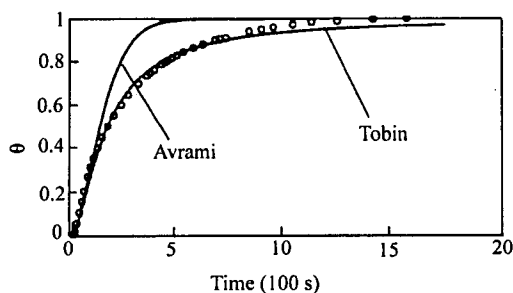


Fig. 6 Predicted time sequence of the transition fraction using Avrami and Tobin models (solid lines). Open circles are experimental results at 72°C.

The crystallization mechanism of the DSPE/glycerol system can be summarized as follows. Nucleation occurs first from the solid metastable lamellar-gel phase and then the nuclei expand immediately over the whole

lamellar plane. The rate-determining step of the crystallization is the growth in the layer-by-layer direction. The growing kinetics is temperature dependent due to the high activation energy, and it is significant at temperatures higher than about 68°C.

## References

- 1 Quinn, P. J. *Cryobiology* **1985**, *22*, 128.
- 2 Yang, L.; Glaser, M. *Biochemistry* **1996**, *35*, 13966.
- 3 Yang, C. P.; Nagle, J. F. *Phys. Rev. A* **1988**, *37*, 3993.
- 4 Takahashi, H.; Hatta, K.; Hatta, I. *J. Phys. II* **1996**, *6*, 1657.
- 5 Cheng, A.; Caffrey, M. *J. Phys. Chem.* **1996**, *100*, 5608.
- 6 Duman, J. G.; Wu, D. W.; Xu, L.; Tursman, D.; Olsen, T. M. *Q. Rev. Biol.* **1991**, *66*, 387.
- 7 Zbylut, J.; Jaskowski, J. M. *Med. Weter.* **1999**, *55*, 516.
- 8 MacDaniel, R. V.; McIntosh, T. J.; Simon, S. A. *Biochim. Biophys. Acta* **1983**, *731*, 97.
- 9 Williams, W. P.; Quinn, P. J.; Tsonev, L. I.; Koynova, R. D. *Biochim. Biophys. Acta* **1991**, *1062*, 123.
- 10 Yu, Z. W.; Tsvetkova, N. M.; Tsonev, L. I.; Quinn, P. J. *Biochim. Biophys. Acta* **1995**, *1237*, 135.
- 11 Avrami, M. *J. Chem. Phys.* **1939**, *7*, 1103.
- 12 Tan, S. S.; Su, A. H.; Li, W. H.; Zhou, E. L. *J. Polym. Sci. B: Polym. Phys.* **2000**, *38*, 53.
- 13 Tobin, M. C. *J. Polym. Sci., Polym. Phys.* **1974**, *12*, 399.
- 14 Tobin, M. C. *J. Polym. Sci., Polym. Phys.* **1976**, *14*, 2253.
- 15 Tobin, M. C. *J. Polym. Sci., Polym. Phys.* **1977**, *15*, 2269.
- 16 Supaphol, P.; Spruiell, J. E. *J. Macromol. Sci. Phys.* **2000**, *B39*, 257.
- 17 MacPherson, A. *Crystallization of Biological Macromolecules*, Gold Spring Harbor Laboratory Press, New York, **1999**, p. 148.
- 18 Eker, F.; Durmus, H. O.; Akinoglu, B. G.; Severcan, F. *J. Mol. Struct.* **1999**, *482*, 693.
- 19 Van Osdol, W.; Johnson, M. L.; Ye, Q.; Biltonen, R. L. *Biophys. J.* **1991**, *59*, 775.